State of the art on the application of waste materials in geopolymer concrete

Case Studies in Construction Materials 15 (2021) e00637

Contents lists available at ScienceDirect

Case Studies in Construction Materials

journal homepage: www.elsevier.com/locate/cscm

Case study

State of the art on the application of waste materials in geopolymer concrete

Z. Podolsky [a], J. Liu [a], H Dinh [a], J.H. Doh [a,*], M. Guerrieri [b], S. Fragomeni [b]

[a] School of Engineering & Built Environment, Griffith University, QLD 4222, Australia
[b] College of Engineering & Science, Victoria University, Cnr Hoadley Ct & Ballarat Rd, Melbourne, VIC 8001, Australia

ARTICLE INFO

Keywords:
Geopolymer concrete
Waste
Fly ash
Strength
Durability

ABSTRACT

This review paper presents and analyses the mechanical and durability properties of geopolymer concrete (GPC) which contain various waste materials. Significant findings have concluded that the absence of guidelines for the mix design of GPC has resulted in a wide variance of design parameters and therefore strength and durability properties. The purpose of this review is to compile recent research to highlight the inadequacy of the current literature and identify areas in which the current mix design can be improved. The development of mix design guidelines that focus on optimal Si/Al ratio, NaOH concentration and sodium silicate to sodium hydroxide (SS/SH) ratio are required, as these factors are significantly affected by the addition of waste materials with varying chemical compositions and morphology.

1. Introduction

1.1. Background

Concrete manufacturing consumes the largest amount of natural resources in the world due to its abundant use of sand, rock and water [1]. Cement production poses significant environmental concerns as a result of greenhouse gas emissions and energy consumption. Specifically, the production of cement accounts for 12–15 % of industrial energy use as well as 5–7 % of all carbon dioxide emissions [2]. Furthermore, it is estimated that the production of 1 t of cement releases approximately 0.85–0.92 t of CO_2 into the environment [3–5]. To reduce these adverse effects, cement can be replaced with waste materials or industrial by-products that possess pozzolanic or self-cementing properties. Commonly used industrial by-products include fly ash, blast furnace slag and silica fume. The use of these materials in concrete reduces the waste associated with their industries while simultaneously reducing the carbon footprint of concrete production. Therefore, the development of sustainable and green concrete that utilises recycled materials is a priority for the construction industry [6–11].

Geopolymer concrete (GPC) is an innovative and environmentally friendly concrete that hardens through the reaction between aluminosilicate waste materials and alkaline activating solutions rather than requiring a cement binder [12]. Precursor materials include fly ash, blast-furnace slag and metakaolin, while alkaline activators consist of chemical compounds such as sodium hydroxide and sodium silicate solution. The reaction between these two base materials facilitates the geopolymer reaction, resulting in a dense, cross-linked polymer structure. A diagram describing the process of geopolymerisation is presented in Fig. 1.

* Corresponding author.
E-mail address: J.doh@griffith.edu.au (J.H. Doh).

https://doi.org/10.1016/j.cscm.2021.e00637
Received 22 April 2021; Received in revised form 15 July 2021; Accepted 21 July 2021
Available online 24 July 2021

From an environmental perspective, GPC enables a reduction in the demand for cement production and provides additional outlets for waste materials and industrial by-products. It is estimated that the use of GPC could reduce energy consumption by up to 43 % and reduce greenhouse gas emissions by 9–80 % compared to cement-based concrete [5,13]. This significant variance is due to the complexity associated with the calculation of emissions which relies on multiple factors including local conditions, transportation and the mix design itself [5]. Furthermore, GPC offers improved durability properties compared to ordinary concrete, such as chloride resistance [14,15], high temperature resistance [16], freeze-thaw cycles [17,18] and carbonation resistance [19]. It has been shown that GPC can have adequate compressive strength [20–22] and tensile strength [23,24].

The use of recycled waste materials in GPC is a developing field. The production of fly ash will cease as a result of the phasing out of coal power plants worldwide by 2040, as stipulated by the Paris Agreement [25]. The significance of this literature review lies in the identification of suitable replacement materials for fly ash while also highlighting the inadequacy of the current state of GPC mix design. This review includes studies on GPC that involve both the partial and complete replacement of fly ash. The merits of each material are analysed in terms of their strength and durability properties, with references to their microstructure and chemical composition to identify areas in which the mix design of GPC can be improved.

1.2. By-product and waste materials

A brief introduction to the various by-product and waste materials discussed in this review follows. Glass is a non-crystalline, amorphous solid material produced through the heating of silica, sodium carbonate and calcium carbonate. From 2016 to 2017,

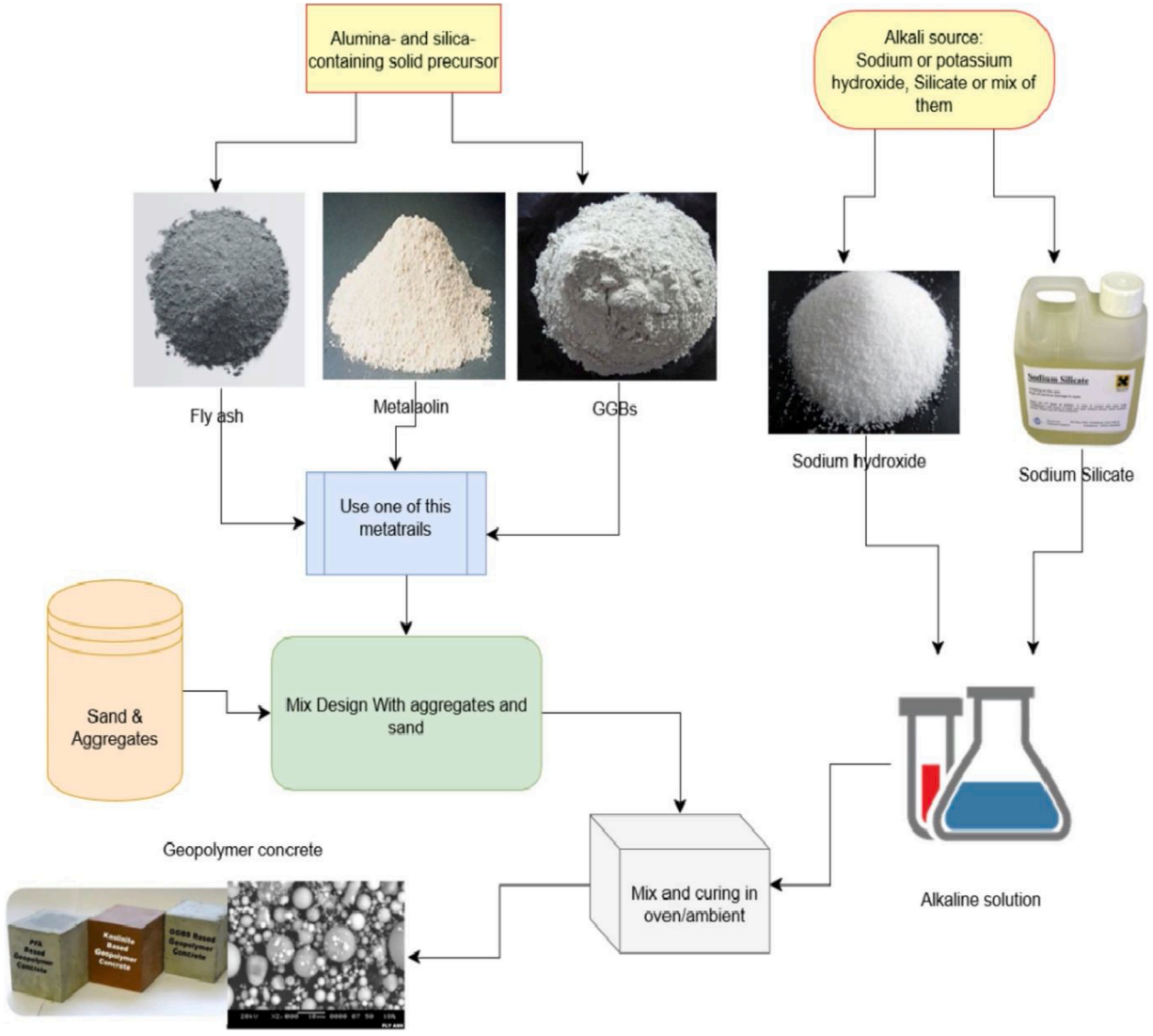

Fig. 1. Geopolymer constituent materials [26].

approximately 1.1 Mt of glass waste were produced in Australia, but only 57 % of it was recycled; the remaining unrecycled glass was disposed of in landfills [27]. This poses a critical environmental problem, as glass is not biodegradable. Therefore, the identification of alternative uses for unrecycled glass waste is important for ensuring future environmental sustainability. Recently, recycled glass has found applications in GPC as a replacement binder material. Waste glass powder (WGP) is a source of silica and alumina; when ground to very fine particle sizes (<150 μm), it can react in the presence of an alkaline solution to facilitate the geopolymer reaction.

Rice husk ash (RHA) is an agricultural waste product of the rice milling industry, which produces approximately 20 million t of it annually. The environmental concerns of RHA are related to the air pollution associated with the combustion of rice husks, as well as its disposal in landfills when alternative solutions exist [28,29]. RHA has a high silica content, which identifies it as a suitable precursor material for GPC. However, its reactivity has been shown to depend on its mineralogy, where amorphous silica phases produce better results than crystalline silica [30].

Ground granulated blast-furnace slag (GGBS) is a by-product of iron production and is produced through the quenching of molten liquid in water. This process produces a fine powder that possesses cementitious properties. GGBS contains a large amount of silica, alumina and calcium content, which makes it a suitable precursor material in GPC.

Metakaolin (MK) is produced through the calcination of natural clays which contain mineral kaolinite at approximately 700–900 °C. It is therefore not a by-product of other industrial processes and is specifically manufactured for use in concrete. Consequently, there is a considerable amount of CO_2 emissions associated with MK production, and it is only widely used in countries where kaolinite is readily available [31]. Nevertheless, MK has high silica and alumina content, which facilitates its use as a fly ash replacement in GPC. While the application of MK is not encouraged, an overview of current research related to it is relevant to this discussion.

Red mud (RM) is a by-product of alumina production, with over 117 million t produced per year. Approximately 85 % of all RM is discarded in landfills, polluting the surrounding environment due to its high alkalinity [32]. RM is a suitable precursor material for GPC owing to its high silica and alumina content.

A ternary diagram depicting the range of chemical compositions for each of the aforementioned materials is presented in Fig. 2. A scanning electron microscopy (SEM) analysis of raw precursor materials shows distinct differences in their microstructures. Fly ash is generally characterised by its smooth and spherical shape, while other waste materials such as slag and WGP have irregular particle shapes, as seen in Fig. 3 [33]. A SEM analysis of RHA and RM reveals angular particles with a range of particle sizes that are varied in shape and porosity [30,34,35]. The wide variation in composition and microstructure results in a diverse range of effects on the finished GPC that will be discussed in this review.

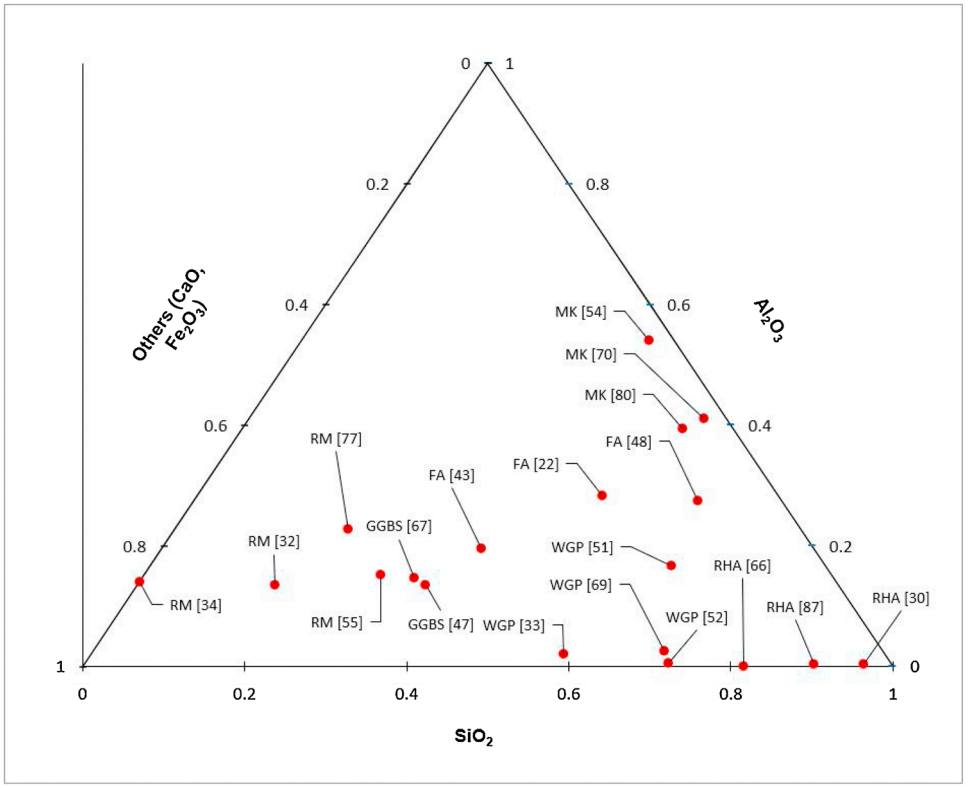

Fig. 2. Chemical composition of each by-product and waste material.

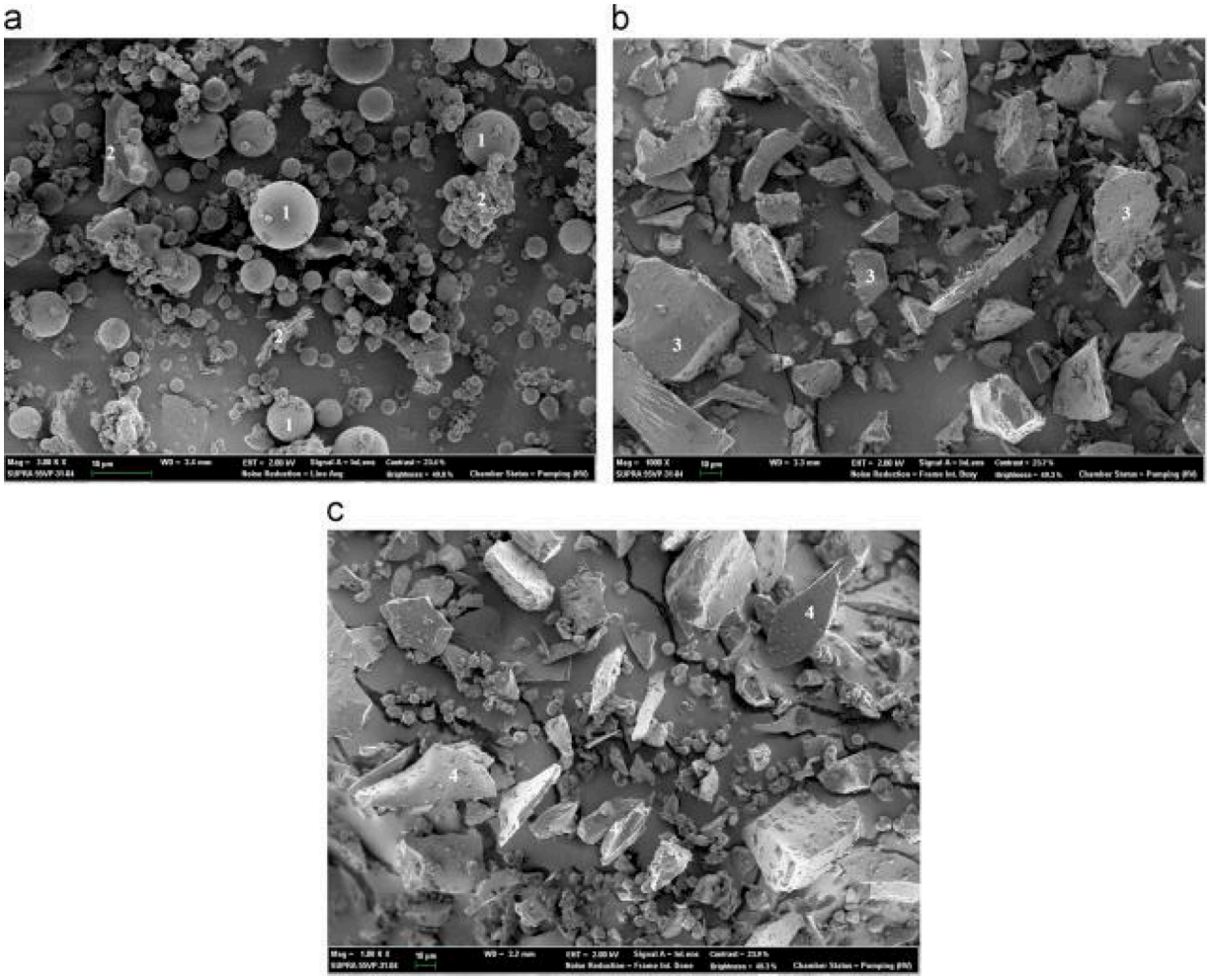

Fig. 3. SEM images of (a) fly ash, (b) slag and (c) waste glass [33].

2. Strength properties

2.1. Workability and setting time

Numerous factors affect the workability of GPC. The rheology of GPC is quite different from that of ordinary concrete due to the high viscosity of sodium silicate solution. Higher sodium silicate to sodium hydroxide (SS/SH) ratios exacerbate this effect, further reducing the mobility of the mixture [22,36,37]. Similarly, an increase in alkali activator concentration tends to reduce workability due to silica and alumina's faster rate of dissolution, which accelerates the geopolymer reaction [38,39]. Additionally, an increase in the volume of activator solution (up to 45 % of binder weight) has been shown to improve workability without significantly impacting the compressive strength of the mixture due to an increase in its liquid-to-solid ratio [22]. However, the application of more activator

Table 1
Initial and final setting time of fly ash-based GPC [40].

Admixtures	Dosage (wt%)	Initial setting time (min)	Final setting time (min)
Control	0	60	130
$CaCl_2$	1	26	60
	2	35	45
$CaSO_4$	1	58	115
	2	56	105
Na_2SO_4	1	82	135
	2	90	130
Sucrose	1	60	210
	2	60	230

solution is not a desirable solution due to the substantial carbon emissions associated with the production of alkali activators [5].

The setting time of GPC strongly correlates with the calcium content of the fly ash. GPC mixtures usually set between one and two hours; however, high calcium content can significantly shorten this time, decreasing setting time by 65 % with 2 % additional calcium content by binder weight, see Table 1 [40]. Furthermore, the dissolution of fly ash happens slowly at room temperature, which results in a slow rate of leaching of silica and alumina; however, calcium leaching is not affected, which increases setting time [41]. This suggests that an understanding of the chemical composition of local fly ash sources is required when designing GPC mixtures. Class F fly ash has low calcium content whereas Class C fly ash has high calcium content. It is therefore recommended to use Class F fly ash if flash setting is a concern. Low sodium hydroxide concentration has been shown to reduce setting time due to the slow leaching of silica and alumina, enabling the reaction with calcium to precipitate more rapidly [22,42,43]. As a solution, the addition of sucrose sugar has a retarding effect on the final setting time of GPC without producing any negative effects on the compressive strength of the concrete [40,44]. The sucrose acts to coat the surface of the precursor materials thus inhibiting the ability of the alkali solutions to bind and precipitate the geopolymer reaction [40].

The application of slag into fly ash-based mixtures results in decreased workability and setting time due to its high calcium content. Numerous studies have identified this phenomenon, which tends to increase the rate of reaction [45–48]. However, the workability of GPC that contains WGP is generally better than that of fly ash-based control mixtures. This improvement in workability can be attributed to the smooth surface and low water absorption of glass [49–51]. However, a reduction in flow has been identified when WGP completely replaces fly ash precursor; this is attributable to the coarse and irregular nature of WGP particles, which reduces the mobility of the mortar [50,52]. When slag is used as a precursor, there is a negligible change in flow due to the similar morphology and structure of WGP and slag [50].

RHA has been shown to decrease the workability of GPC which contains fly ash, as seen in Fig. 4. This can be attributed this to the difference in shape between fly ash and RHA particles, which are spherical and angular, respectively [30]. Additionally, water can be stored in pores, causing the mixture to become more cohesive [30,53]. Furthermore, RHA has a high water requirement due to the absorption characteristics of the RHA particles. Insufficient water content can result in more rapid hardening and thus decreased workability and setting time [53].

The literature on the workability and setting time of MK- and RM-based GPC is limited. An increase in MK content tends to improve workability due to the smooth morphology and small particle size of MK [20,54]. MK also increases the setting time of slag- and fly ash-based GPC by approximately 15 % due to its low calcium content [20,54]. Similarly, the addition of RM to fly ash-based GPC increases setting time, as shown in Fig. 5 [55].

The setting time of MK-based GPC increases significantly with the addition of WGP from 615 min to 1,245 min at 40 % replacement [56]. WGP has a smaller surface area than MK due to its larger particle size, which reduces the amount of reactive content for the activator solution. This reduces the dissolution rate of silica and alumina and results in increased setting time [49]. Fig. 6 demonstrates the increase in setting time associated with additional WGP replacement.

2.2. *Compressive and tensile strength*

The primary parameters which affect the strength properties of GPC are alkaline liquid to binder (AL/B) ratio, the type and concentration of alkali solution and the molar ratio of SiO_2 to Na_2O. While the exact effect of each of these parameters on GPC is not fully understood, there are some well-accepted properties [57,58]:

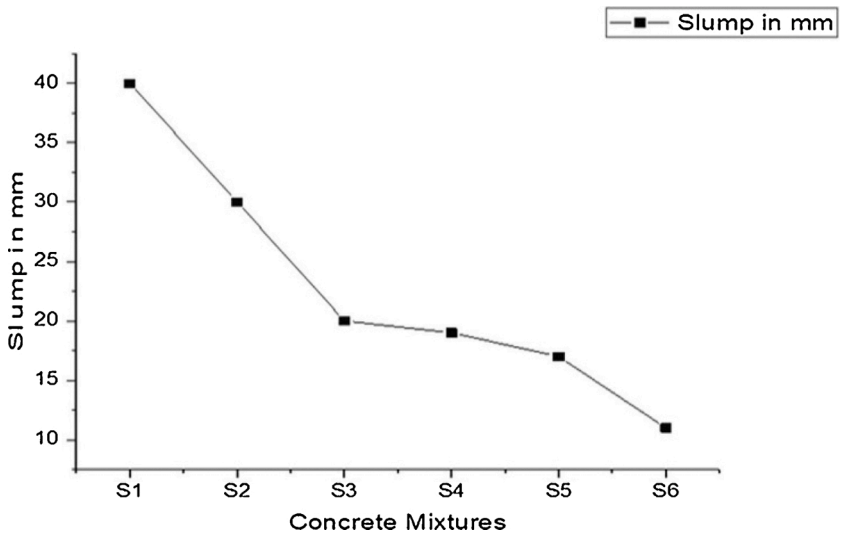

Fig. 4. Workability of GPC containing RHA [30].

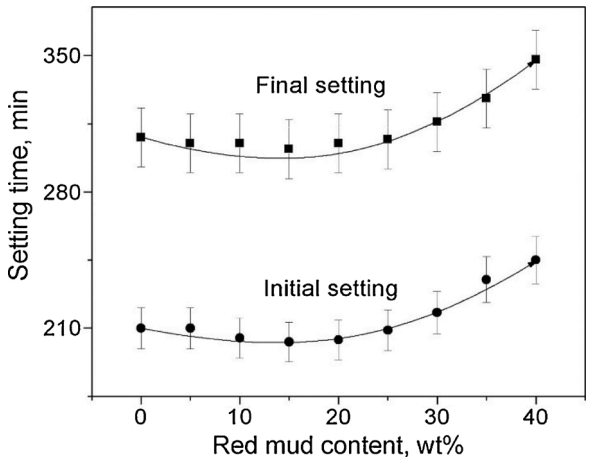

Fig. 5. Initial and final setting time of GPC containing red mud [55].

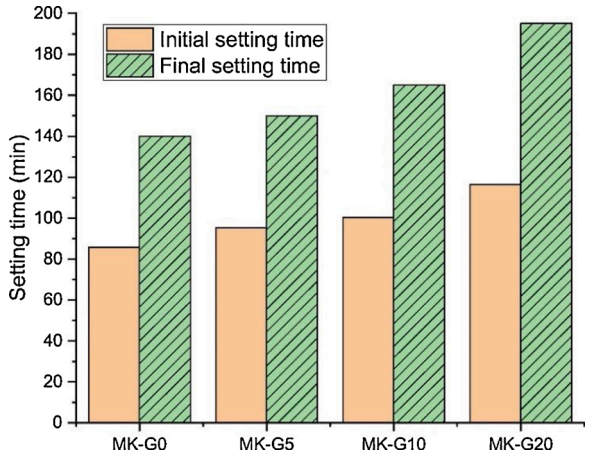

Fig. 6. Setting time of MK-based GPC with WGP replacement [49].

1 Increasing AL/B decreases strength.
2 Increasing the molarity of alkaline activators increases strength.
3 The optimal molar ratio of SiO_2 to Na_2O is approximately 1.0–2.0.

In GPC, AL/B ratio is a critical factor in determining its strength and workability; therefore, the type, amount and concentration of the alkaline activator must be considered [59]. High alkali concentration generally correlates with improved compressive strength [60,61]. However, excessive molarity can reduce ion mobility, which slows the geopolymer reaction [62]. Additionally, the AL/B ratio controls the amount of liquid in the mix, such that lower values produce stronger concrete due to the relative increase in binder content; this phenomenon is highlighted in Fig. 7 [63,64].

Another important factor in the design of GPC is the SS/SH ratio. There are numerous conflicting studies on the optimal ratio of AL/B and SS/SH, which range from 0.4 to 0.45 and 1.5 to 2.0, respectively [22,63]. Fig. 8 demonstrates the relationship between AL/B, SS/SH and compressive strength. The compressive strength of GPC mixes tends to increase with SS/SH until a certain maximal point, after which it decreases. This can be attributed to an increase in Si-O bonds that significantly improve the strength of the GPC, while excess, unreacted silica prevents water evaporation and structure formation, reducing the strength of the geopolymer [49,63,65].

Prolonged exposure to high curing temperatures as well as the presence of excessively alkaline solutions can cause the disintegration of the geopolymer gel, an effect which is demonstrated in Fig. 9 [66]. Similarly, pores and voids can result from the presence of air bubbles during the mixing and casting process and the evaporation of water during the curing process [34,35,67]. Additionally, cracks can result from shrinkage due to high temperature curing and applied stress during compression tests [34,68].

The compressive strength of GPC that contains WGP is varied and inconclusive. As seen in Fig. 10, compressive strength is greatest at 12.5 % WGP replacement, regardless of NaOH concentration [69]. Other studies have shown various optimal replacement percentages ranging from 5 % [49] to 50 % [66]. As Si-O-Si are the strongest bonds, it is expected that an increase in silica-to-alumina ratio would improve the strength of the concrete [33,70]. However, further addition of WGP results in a decrease in compressive strength.

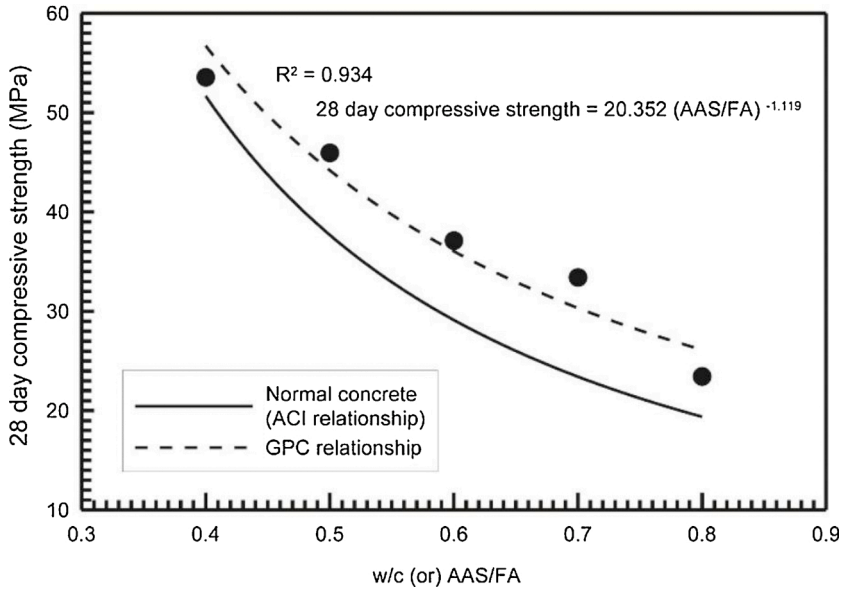

Fig. 7. Effect of AL/B on the compressive strength of GPC [64].

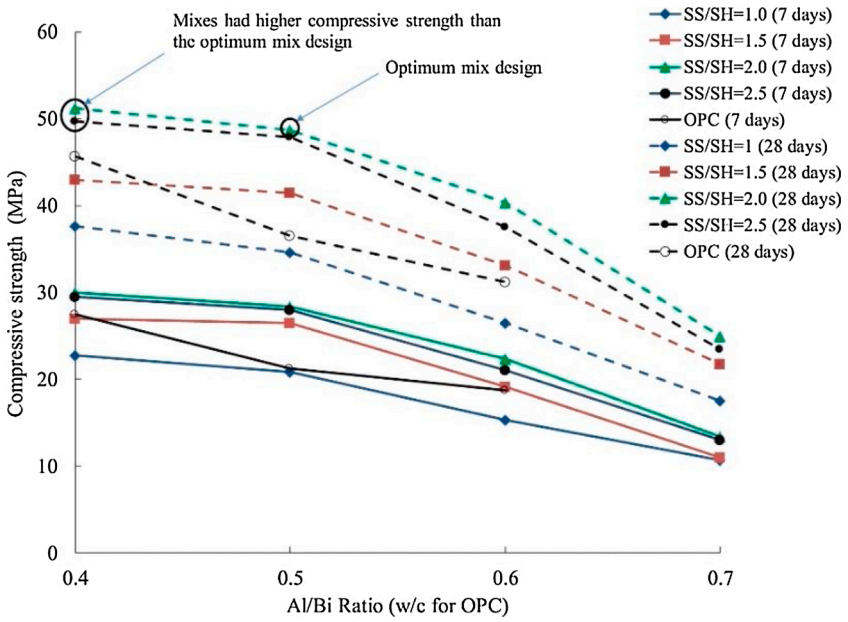

Fig. 8. Effect of AL/B and Na2SiO3/NaOH (SS/SH) on the compressive strength of GPC [63].

This is due to a reduction in the release rate of silica and alumina ions, which results from the slow rate of dissolution of WGP [69]. Further increases in WGP content result in a larger number of unreacted glass particles, thus decreasing the potential of the geopolymer reaction [56,69]. Therefore, the high silica content of WGP can result in decreased strength beyond an optimal replacement percentage. Furthermore, excessive silica content can decrease the amount of sodium in the binder, thus reducing the formation of the N-A-S-H gel that is responsible for the formation of a compact and dense microstructure [45,49,71].

Although longer curing times tend to increase the compressive strength of GPC, it is notable that, beyond 12.5 % replacement, compressive strength has been reported to decrease at 28 days compared to seven days [69]. This loss in strength can be attributed to a change in morphology and an increase in the porosity of the geopolymer over time when the WGP content exceeds 25 % [72]. Additionally, SEM micrographs have identified sodium-rich porous areas, which potentially resulted from the production of sodium-silicate gel instead of aluminosilicate gel [73]. It is notable that the excessively high alkalinity of NaOH can cause the disintegration of the geopolymer gel [66].

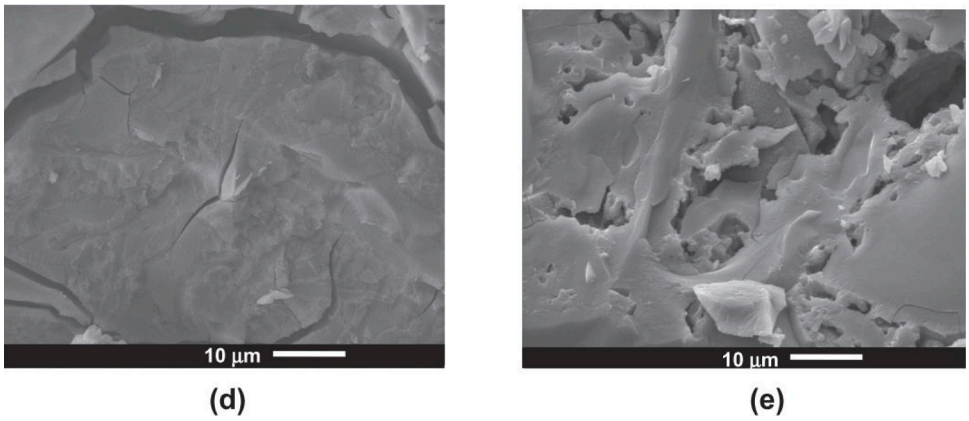

Fig. 9. SEM of WGP-based GPC under (d) heat curing for 24 h and (e) heat curing for 48 h [66].

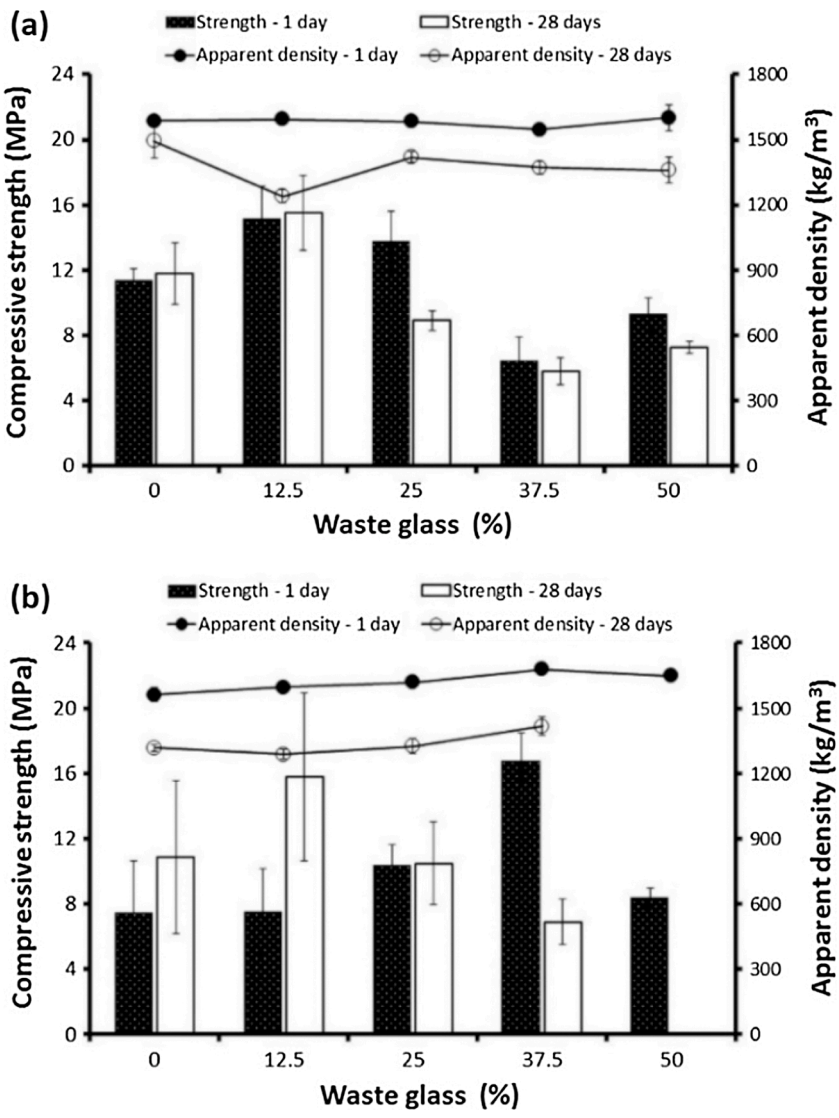

Fig. 10. Density and compressive strength of GPC with WGP replacement of MK using (a) 10 M and (b) 12 M NaOH solution [69].

The effects of RHA replacement in GPC are equally variable. In slag-based GPC, the compressive (see Fig. 11) and tensile strength of the concrete increases up to 15 % replacement, then decreases beyond that point [67]. The same trend can be observed in fly ash-based GPC where the optimal replacement percentage is 35 % (see Fig. 12(b)) [35].This improvement in strength can be attributed to the additional silica content provided by the RHA as well as its smaller particle size compared to slag, which increases the surface area available for the reaction [34,38,67,74]. The addition of RHA further amplifies the number of Si-O-Si bonds, thus strengthening the geopolymer [33,34,70]. However, a corresponding decrease in strength with further RHA replacement can occur due to oversaturation of unreacted RHA particles and silica content, which hinder the formation of geopolymer structures [35]. Furthermore, the differences in solubility between RHA and slag can cause a reduction in the rate and extent of geopolymerisation [67,75].

By contrast, some studies have demonstrated that the compressive strength of RHA groups was lower even at 10 % RHA replacement compared to the control. This sharp decrease in strength is attributable to the low quantity of alumina in RHA, which causes an imbalance in the Si/Al ratio of the precursor materials [30]. Above a concentration of 10 M, the compressive strength of RHA-based GPC has been reported to decrease, as shown in Fig. 12(a) [35]. This conflicts with numerous earlier studies that showed an increase in compressive strength associated with increased sodium hydroxide concentration, which resulted from the greater dissolution of silica and alumina in more concentrated solutions [34,38]. The decrease in compressive strength can be explained by the higher viscosity of the 12 M and 14 M sodium hydroxide solutions, which prevents the silica and alumina from reacting, as well as excess hydroxide ions, which form aluminosilicate gel at early stages and reduce the effectiveness of geopolymerisation [34,35].

MK replacement in slag-based GPC can improve compressive strength; however, this effect is diminished at 50 % or greater replacement. This can be attributed to the greater silica content of slag compared to MK, which is alumina-rich [54]. However, other studies found the opposite result, in which the addition of MK significantly decreased strength at any replacement. This strength loss can be explained by the decrease in calcium content associated with smaller proportions of slag, which causes a delay in the geopolymer reaction [46,48,76]. This relationship is demonstrated in Fig. 13, which shows a reduction in strength with fly ash replacement compared to the 100 % slag-based control GPC. Furthermore, slag replacement increases early age strength and results in fast setting times due to the rapid formation of calcium-silicate gel [47].

There have also been conflicting reports on the effects of adding RM to GPC. Some studies have identified decreased compressive strength due to the low silica content of RM, which reduces the number of strong Si-O bonds in the mixture [77]. However, this can be attributed to the particle size of RM (stated as <100 μm), which is small relative to the base precursor material [77]. On the other hand, there have been reports of increased strength up to 50 % replacement of slag with RM [32]. One study found an increase in strength in fly ash-based GPC with RM replacement up to 10 %, then a decrease in strength with additional replacement (see Fig. 14). This can be attributed to the achievement of an optimal ratio of Si/Al ions for the geopolymer reaction [55].

At optimum replacement of slag with RHA, SEM micrographs show GPC that is characterised by a compact and dense microstructure due to the presence of calcium hydration products [35,67]. SEMs indicate that the geopolymerisation reaction occurs in both fly ash and RHA; however, increased magnification indicates the existence of unreacted particles. Specifically, the structure of the 8 M NaOH geopolymer in Fig. 15 consisted of large particles with excessive gaps, while the 10 M geopolymer had a denser structure [35]. The 12 M and 14 M samples had large numbers of unreacted silica particles on the surface, which explains the corresponding reduction in compressive strength. Additional RHA replacement leads to an oversaturation of silica content, resulting in the presence of unreacted silica and a more porous microstructure [35,67].

Table 2 summarises recent research on the compressive strength of GPC that contains waste materials. There is a notable spread in particle size, optimal replacement percentage and maximum strength. The lack of clear guidelines for the mix design of GPC has led to widely varying results even when similar parameters were tested, with compressive strength ranging from 15.5 MPa to 72 MPa.

2.3. Elastic modulus

There is limited literature on the elastic modulus of GPC which contains waste materials. The elastic modulus of GPC is generally low; however, this is not a rule as the mechanism is not well understood. There is some variance in reported values, which range from

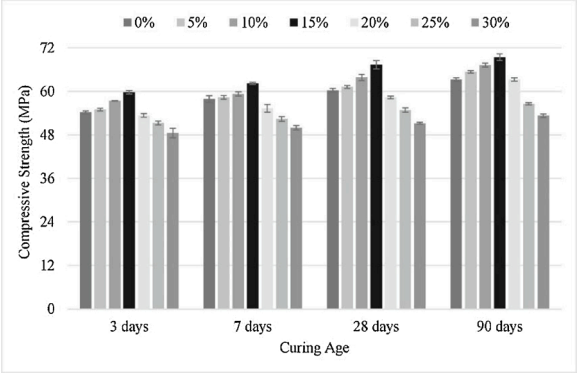

Fig. 11. Compressive strength of GPC containing RHA [67].

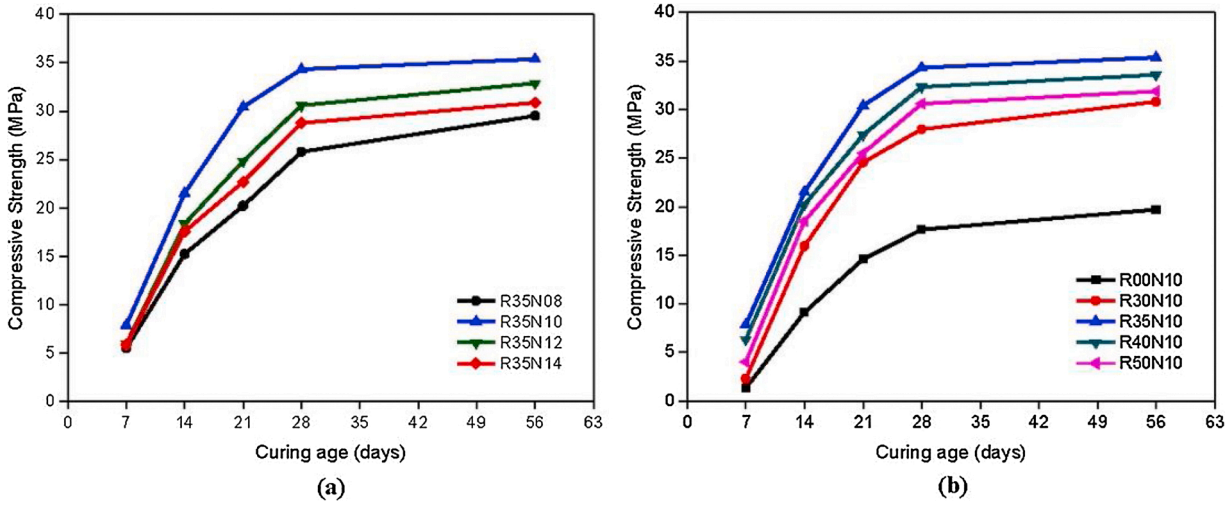

Fig. 12. Compressive strength of GPC containing RHA [35].

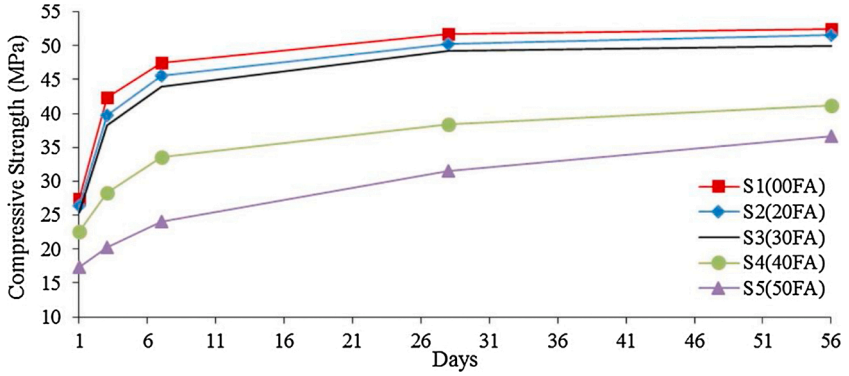

Fig. 13. Compressive strength of slag-based GPC with FA replacement [46].

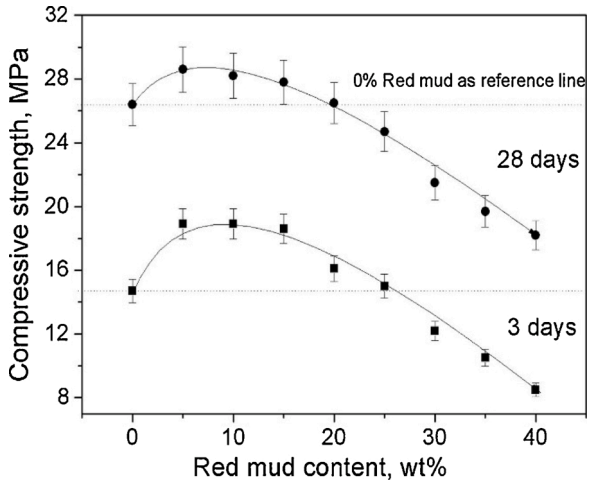

Fig. 14. Compressive strength of FA-based GPC with RM replacement [55].

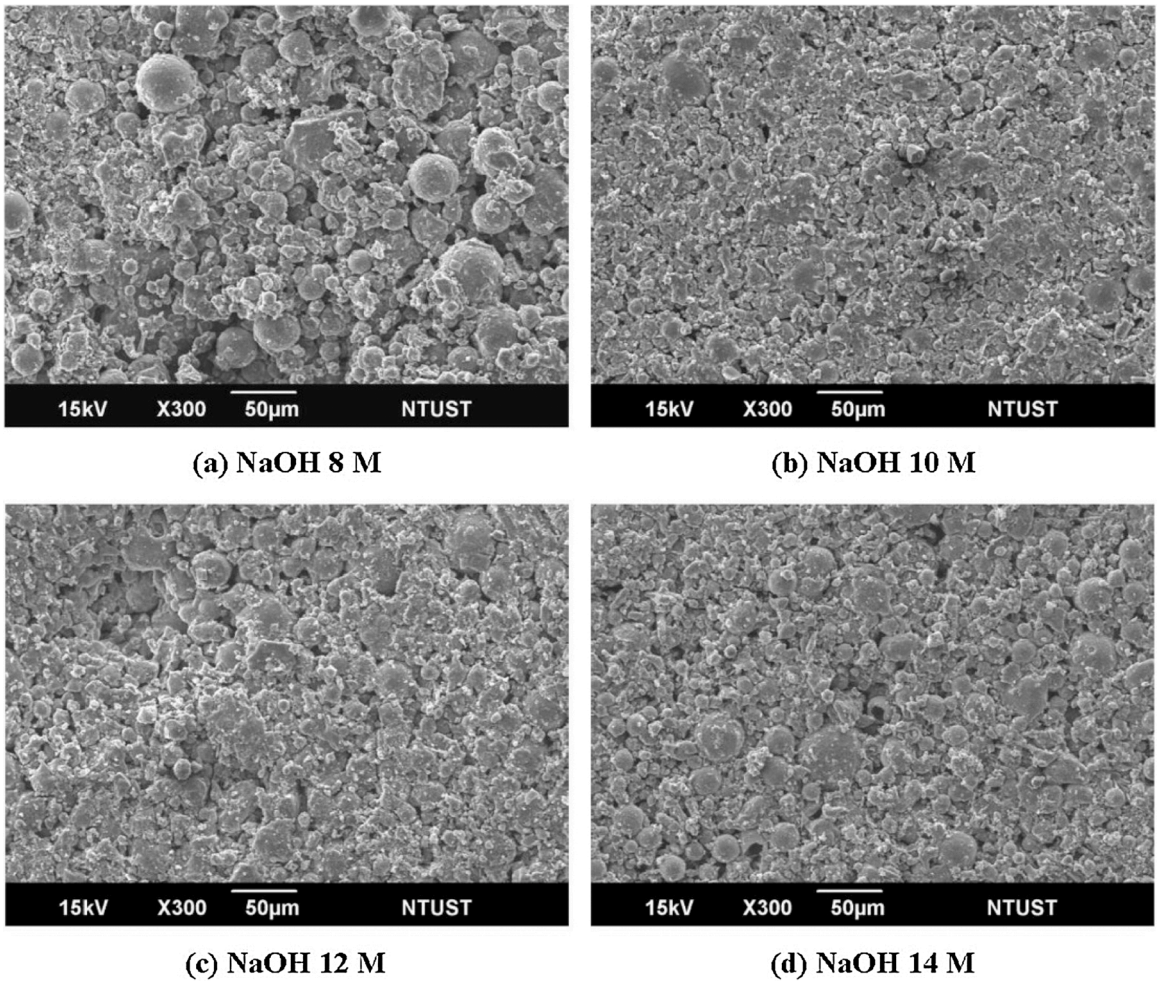

Fig. 15. SEM of GPC containing RHA, the effect of NaOH Concentration [35].

Table 2
Summary of literature on the compressive strength of GPC containing waste materials.

Base Precursor	Replacement Material	Particle Size of Replacement Material (μm)	Optimal replacement (%)	Maximum strength (MPa)	Source
FA	WGP	<74	10	19.24	[33]
FA	WGP	30	20	25.68	[78]
FA	WGP	47.9	30	28	[50]
MK	WGP	<75	12.5	15.5	[69]
MK	WGP	13	5	35	[73]
FA	WGP	20	50	35	[66]
MK	WGP	7.5	5	41	[49]
Slag	RHA	10.73	10	25	[30]
RM	RHA	<150	50	20.5	[34]
FA	RHA	10	35	35.4	[35]
FA	RHA	8.3	10	28.4	[79]
FA	RHA	16.76	3	72	[75]
MK	RHA	12.5	30	57	[80]
Slag	RHA	7	15	69.4	[67]
FA	MK	3.5	40	51	[41]
Slag	FA	–	20	58	[46]
FA	Slag	23	100	64	[47]
Slag	MK	–	30	51.16	[54]
Slag	RM	<100	30	48	[77]
Slag	RM	–	50	52	[32]
FA	RM	1.57	10	30	[55]

as high as 23.0–30.8 GPa [58] to as low as 10.70–18.4 GPa [81]. Therefore, GPC is more ductile due to its low elastic modulus. However, the elastic modulus can be increased by using more highly concentrated activating solutions [82,83]. Critically, elastic modulus tends to correlate with compressive strength; this trend can be observed in Fig. 16 [84,85]. Furthermore, there is a negligible difference in elastic modulus when fly ash is replaced with slag up to 60 % [84].

MK-based GPC also has low elastic modulus but high compressive strength, which can be attributed to the dense polymerised crosslinked network associated with geopolymerisation [68]. The replacement of MK with WGP in MK-based GPC shows improved elastic modulus, which can be attributed to the increase in silica-to-alumina ratio; this results in a denser gel structure at higher replacement percentages due to the increase in the number of strong Si-O bonds in the mixture [49,65]. However, a decrease in elastic modulus above a certain replacement percentage can be explained by the weak bond between the gel phase and the smooth surface of the unreacted WGP [49,52]. Fig. 17 illustrates the relationship between elastic modulus and various contents of MK precursor.

It has been reported that low percentage replacements of MK in slag-based GPC result in higher elastic moduli. This is due to the more rapid hydration of slag due to its high calcium content and the added stiffness associated with slag, whereas MK is associated with plasticity [54]. The replacement of RM with RHA in RM-based GPC shows a correlation between compressive strength and elastic modulus. However, elastic moduli as low as 0.76–1.89 GPa have been reported [34]. Thus, further research on the elastic modulus of GPC which contains waste materials is recommended.

Table 3 summarises the literature on the strength properties of GPC which include waste materials

3. Durability properties

3.1. Alkali-silica reaction

The incidence of the alkali silica reaction (ASR) in GPC is significantly less of a concern than in cement-based concrete [88–90]. This is due to the presence of alumina in the pore solution which prevents the dissolution of the silica in the aggregates that would be responsible for the expansion [91]. Notably, alkali activation is a necessary component of the geopolymer reaction that strengthens the concrete. However, alkali activation of silica content does not cause the expansion of GPC, ASR is only a concern when the aggregate is alkali reactive [90–92]. Furthermore, it has been observed that a worst-case scenario involving the use of highly reactive aggregates and a high concentration of alkali activator resulted in only 5 % of the expansion seen in equivalent ordinary concrete [90]. Fig. 18 displays an overview of the expansion of GPC over time due to ASR.

ASR occurs more commonly in concretes with large glass particles, as glass is a source of amorphous silica which directly facilitates the reaction [93–96]. There have been significant cracks in concretes with a large percentage of glass replacement, which could be the result of ASR. However, the presence of these cracks has also been attributed to other factors, such as the irregular shape and change in morphology of the glass (see Fig. 3), weak bond strength between the glass and matrix, and an increase in porosity arising from unreacted silica [50,69]. Further research on this topic is recommended.

3.2. Acid resistance

Generally, GPC is less susceptible to chemical attack than ordinary concrete due to a lack of reactivity between aluminosilicate oxides and alkali activators with sulphate [97]. Furthermore, fly ash-based GPC performs well in sulphate environments due to its stable and crosslinked aluminosilicate polymer structure and its inherently low calcium content [98]. However, there are conflicting reports regarding the effectiveness of GPC in resisting chloride attack. It has been reported that fly ash-based GPC is highly resistant to chloride ingress [71], that its chloride resistance is the same as ordinary concrete [99] and that it has higher chloride penetration [100]. However, bulk diffusion tests have found a high chloride content as deep as 25 mm from the surface, which indicates low resistance to chloride diffusion due to the GPC's low binding capacity and interconnected pore structures [101].

The use of WGP has been shown to result in a less porous concrete due to the strengthening of its microstructure, which improves its resistance to acid attack by reducing permeability [102–104]. Similarly, it has been shown that increasing the amount of WGP

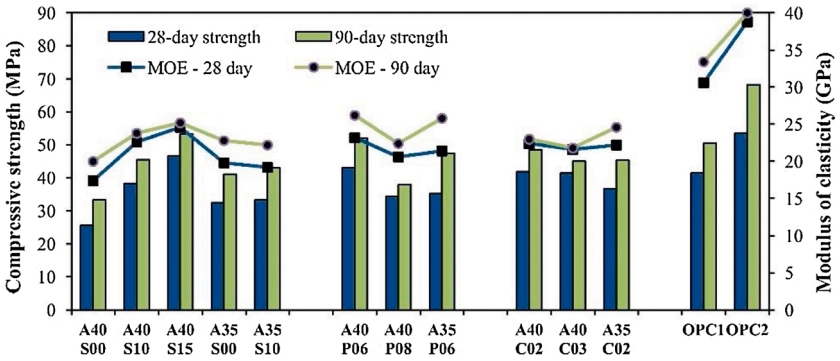

Fig. 16. Comparison between compressive strength and elastic modulus of FA-based GPC with slag replacement and OPC [84].

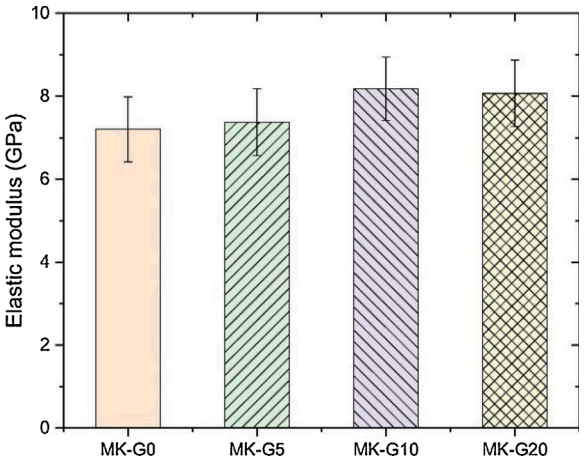

Fig. 17. Elastic modulus of GPC containing MK precursor replacement by WGP [49].

Table 3
Summary of literature on the strength properties of GPC with waste materials.

Base Precursor	Replacement Material	Particle size (D_{50})	Experimental parameters	Strength properties tested	References
FA, slag	WGP	<74 μm	% rep (10, 20, 30), 10 M NaOH, SS/SH = 1.5	Compressive strength	[33]
FA, RM	WGP	<75 μm	% rep (10, 20, 30), 10 M NaOH	Compressive strength	[86]
MK	WGP	–	% rep (10, 20, 30, 40), 10 M NaOH, Si/Na (0.8–2.0), solid/liquid (0.4–1.0),	Compressive strength, workability, setting time	[56]
FA, slag	WGP	30 μm	%rep (20), 8 M NaOH	Compressive strength, workability, setting time	[78]
FA, slag	WGP	47.9 μm	% rep (30 % slag,100 % FA), 10 M NaOH	Compressive strength, workability	[50]
MK	WGP	<75 μm	% rep (12.5, 25, 37.5, 50), 10 M & 12 M NaOH	Compressive strength, workability	[69]
MK	WGP	13 μm	% rep (5, 8), 5 M, 8 M & 10 M NaOH	Compressive strength,	[73]
MK	WGP	7.5 μm	% rep (5, 10, 20), 15 M NaOH	Compressive strength, workability, setting time, elastic modulus	[49]
Slag	RHA	10.73 μm	% rep (1, 3, 5, 7, 10), 10 M NaOH, SS/SH = 2.0	Compressive strength, workability	[30]
RM	RHA	<150 μm	% rep (30, 40, 50, 60), 2 M, 4 M & 6 M NaOH	Compressive strength, elastic modulus	[34]
FA	RHA	–	% rep (0–50), 8–14 M NaOH	Compressive strength	[35]
RHA	Slag	–	% rep (5, 10), 16 M NaOH, SS/SH = 2.5	Compressive strength	[87]
FA	RHA	8.3 μm	% rep (10, 15, 25), 5 M NaOH, SS/SH = 2.5	Compressive strength	[79]
FA	RHA	16.76 μm	% rep (3, 7), 8 M NaOH, SS/SH = 2.5	Compressive strength	[75]
MK	RHA	12.5 μm	% rep (10, 20, 30, 40), 12 M NaOH, SS/SH = 1.5	Compressive strength	[80]
Slag	RHA	7 μm	% rep (5, 10, 15, 20, 25, 30), 10 M NaOH, SS/SH = 2.5	Compressive strength, tensile strength	[67]
FA	RHA	13.9 μm	% rep (1.2, 2.4, 3.6), 8 M, 12 & 16 M NaOH, SS/SH = 1.9–2.0	Compressive strength, tensile strength, flexural strength	[39]
FA	MK	3.5 μm	% rep (30, 40, 50, 60, 70), 5 M NaOH	Compressive strength	[41]
Slag	MK	–	% rep (30, 50), 8 M NaOH, SS/SH = 2.5	Compressive strength, workability, elastic modulus	[54]
Slag	RM	<100 μm	% rep (30, 50), SS/SH = 3.0	Compressive strength	[77]
Slag	RM	–	% rep (12.5, 25, 50), 6 M NaOH	Compressive strength	[32]
FA	RM	1.57 μm	% rep (5, 10, 15, 20, 25, 30, 35, 40), 6 M NaOH	Compressive strength, setting time	[55]
FA	Slag	–	% rep (20, 40, 60), 14 M NaOH, SS/SH = 2.5	Compressive strength, flexural strength, elastic modulus	[84]

replacement in slag-based GPC results in less deterioration when the concrete is submerged in sulphate solution (see Fig. 19; Wang et al., 2017). This can be attributed to the development of a denser microstructure resulting from the fine particle sizes of the glass and precursor material [51,98]. However, 100 % glass replacement has been shown to result in approximately 38 % and 45 % more deterioration compared to control specimens after submersion in chloride and sulphate solutions, respectively [105]. Fly ash-based GPC exhibits significantly higher corrosion rates when immersed in chloride solution compared to equivalent Portland cement concrete. This can be attributed to a reduction in the pH of the pore solution in the geopolymer backbone due to the presence of hydroxide ions, which increases the Cl^-/OH^- ratio [15].

The sorptivity and chloride permeability of RHA-based GPC improves steadily up to an optimal replacement percentage, beyond which the properties start to worsen, as can be observed in Fig. 20 [67]. Similarly, the presence of RHA can increase the concrete's

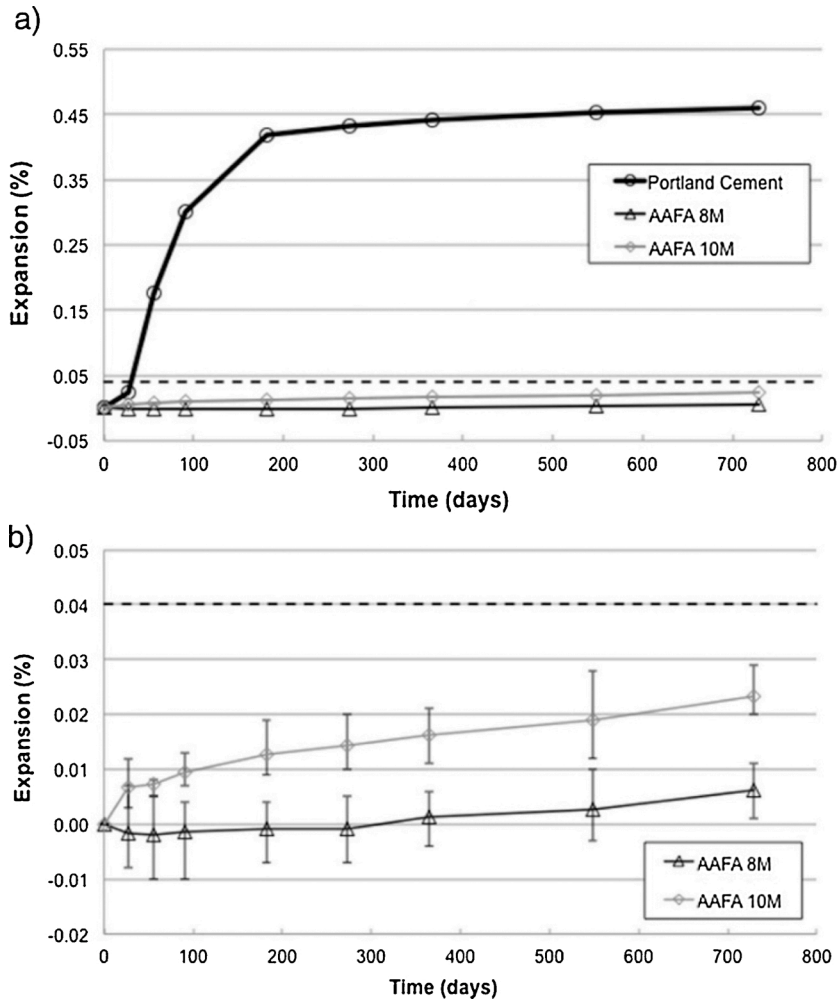

Fig. 18. Expansion over time due to ASR in GPC [90].

resistance to water penetration, decreasing the depth of penetration by up to 13 % compared to a control [87]. This can be explained by the fineness of RHA particles, which result in a denser microstructure [67,87]. However, with further RHA replacement, the pores and voids associated with excess unreacted silica content result in a weaker matrix that is less resistant to permeable ions. Additionally, MK-based GPC has a lower corrosion rate in a chloride environment compared to ordinary concrete, that can be explained by its high alumina content which acts to fill excess pores, resulting in a less permeable concrete [106]. Table 4 summarises the literature on the durability properties of GPC concrete that incorporates waste materials.

4. Conclusion

The application of alternative waste materials in GPC to partially or fully replace fly ash is a developing field. This paper reviewed all the recent literature on this topic. The findings of this review, including recommendations for future research, can be summarised as follows:

- Setting time is a function of the calcium content in the GPC mixture, with high calcium accelerating the rate of reaction. It is therefore critical to perform an analysis of the chemical composition of the base materials to determine whether a retarder is necessary. This is primarily a concern when using slag due to its naturally high calcium content. However, fly ash has variable calcium content, depending on its source. Sugar has been used as a suitable retarder, but more research is required to identify a commercially available solution for GPC mixtures.
- Workability is dependent on the shape, size and general morphology of particles in waste materials. Fly ash, MK and RM particles are smooth and spherical, resulting in acceptable workability, whereas WGP, RHA and slag particles are coarse and irregular, resulting in reduced workability.

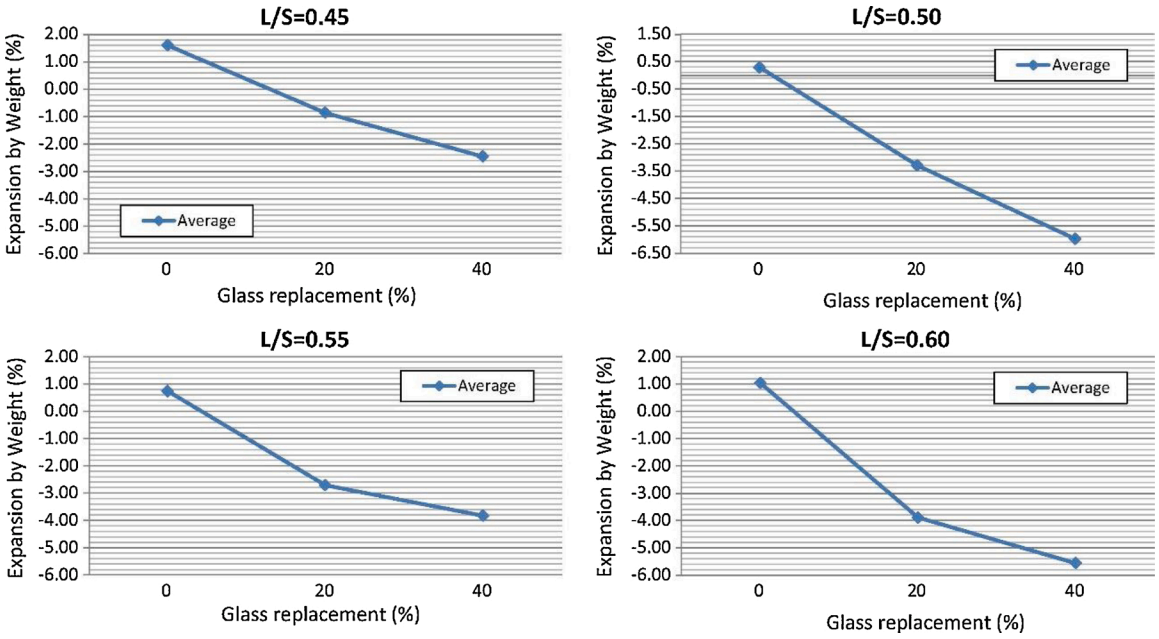

Fig. 19. Expansion by weight of sulphate attack in GPC containing WGP [51].

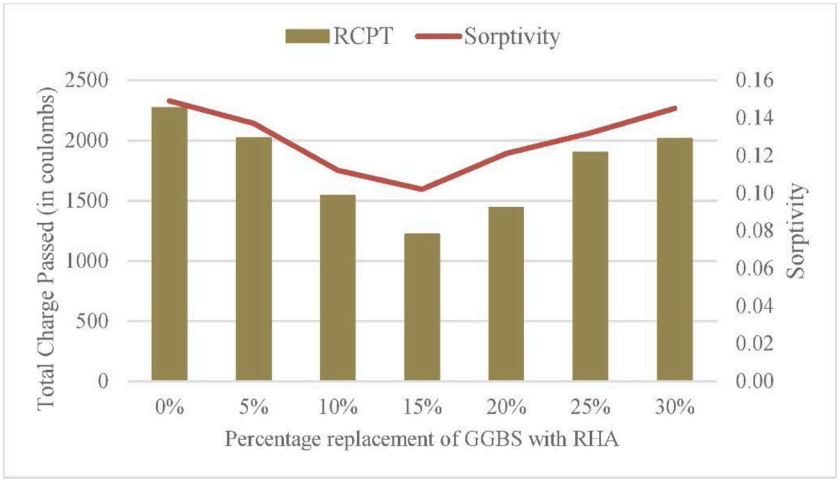

Fig. 20. Chloride penetration and sorptivity of GPC containing RHA [67].

- All waste materials have been successfully applied in GPC, and a wide variety of compressive strengths have been reported in the literature, with values ranging from 15.5 to 72 MPa. Table 2 summarises the literature on compressive strength and optimal replacement percentages.
- Compressive strength can be improved with the replacement of fly ash with other waste materials; however, it is strongly dependent on the mix design, which highlights the importance of Si/Al ratio, NaOH concentration and SS/SH ratio as factors. It is critical to note that there are no official standards or guidelines for the development of GPC, which further exacerbates this uncertainty. Further research on optimal mix design parameters is necessary to establish a methodology for consistent strength development.
- GPC is a ductile material due to its inherently low elastic modulus. This property remains unchanged with the addition of alternative waste products, and it has been shown to correlate strongly with the compressive strength of the GPC.
- SEM enables the imaging of microstructures, including the identification of the morphology of waste materials and the overall microstructure of the finished concrete. Compact and dense microstructures are seen in samples with high compressive strength, while unreacted particles that cause pores and voids are also present and observable. SEM is an important tool for understanding the effects of waste materials on GPC, and its use is recommended in all cases.

Table 4
Summary of literature on the durability properties of GPC with waste materials.

Base Precursor	Replacement Material	Particle size (D_{50})	Experimental parameters	Durability properties tested	References
FA	–	45 μm	Steel fibres (0.25 %, 0.5 %, 0.75 %, 1.0 %), 10 M NaOH, SS/SH = 2.0	Water absorption, abrasion, acid resistance, sulphate resistance, bulk diffusion	[99]
FA	–	–	15 M NaOH, SS/SH = 2.6–8.7	Water absorption and permeability, chloride resistance	[71]
MK	–	8 μm	10 M, 12 M NaOH, SS/SH = 1.5–1.9	Chloride resistance,	[106]
Slag	–	–	3 %, 5 %, 7 % & sulphate solution, SS/SH = 2.5	Sulphate resistance	[98]
FA/slag	WGP	<75 μm	8 M NaOH, SS/SH = 2.0	Sorptivity, porosity, chloride penetration	[104]
FA	–	–	14 M NaOH, SS/SH = 1.0	ASR	[88]
FA	MK	–	% rep (20, 30, 40), 14 M NaOH, SS/SH = 2.5	Acid resistance, sulphate resistance	[97]
FA	–	6–30 μm	12 M NaOH	Chloride resistance,	[101]
FA	–	–	14 M NaOH, SS/SH = 2.0,2.5	Porosity, chloride resistance	[100]
FA	–	–	4 M, 6 M, 7 M, 8 M, 9 M, 10 M, 11 M NaOH	ASR	[90]
FA	–	–	SiO2/Na2O = 1.4	ASR	[91]

- ASR is generally not a problem for GPC. However, the high silica content of WGP and RHA is a concern. There is evidence of cracks occurring in concretes with high percentages of these materials. Thus, further investigation is recommended.
- The application of waste materials has varying effects on the acid resistance of GPC. The presence of WGP and RHA tend to reduce permeability, as they do not absorb water; there is evidence that this occurs in fly ash- and slag-based geopolymers, which results in improved sulphate resistance. Similarly, the high alumina content of MK can improve chloride resistance. However, the literature on this topic is limited, and more research is recommended.

Declaration of Competing Interest

None

References

[1] P.K. Mehta, Greening of the concrete industry for sustainable development, Concr. Int. 24 (2002) 23–28.
[2] F.N. Stafford, A.C. Dias, L. Arroja, J.A. Labrincha, D. Hotza, Life cycle assessment of the production of Portland cement: a Southern Europe case study, J. Clean. Prod. 126 (2016) 159–165, https://doi.org/10.1016/j.jclepro.2016.02.110.
[3] Environmental Protection Agency, Available and Emerging Technologies for Reducing Greenhouse Gas Emissions From the Nitric Acid Production Industry, 2010, p. 31. http://www.epa.gov/sites/production/files/2015-12/documents/nitricacid.pdf.
[4] B.H.G. Van Oss, G.A. Norton, U.S.G. Survey, Background Facts and Issues Concerning Cement and Cement Data, U.S. Department of the Interior, 2005, p. 88. http://www.usgs.gov.
[5] V. Shobeiri, B. Bennett, T. Xie, P. Visintin, A comprehensive assessment of the global warming potential of geopolymer concrete, J. Clean. Prod. 297 (2021) 126669, https://doi.org/10.1016/j.jclepro.2021.126669.
[6] A. Arulrajah, M.M. Disfani, H. Haghighi, A. Mohammadinia, S. Horpibulsuk, Modulus of rupture evaluation of cement stabilized recycled glass/recycled concrete aggregate blends, Constr. Build. Mater. 84 (2015) 146–155, https://doi.org/10.1016/j.conbuildmat.2015.03.048.
[7] S. Lotfi, M. Eggimann, E. Wagner, R. Mróz, J. Deja, Performance of recycled aggregate concrete based on a new concrete recycling technology, Constr. Build. Mater. 95 (2015) 243–256, https://doi.org/10.1016/j.conbuildmat.2015.07.021.
[8] F. López-Gayarre, R. Blanco Viñuela, M.A. Serrano-López, C. López-Colina, Influence of the water variation on the mechanical properties of concrete manufactured with recycled mixed aggregates for pre-stressed components, Constr. Build. Mater. 94 (2015) 844–850, https://doi.org/10.1016/j.conbuildmat.2015.07.097.
[9] F. Liu, L.Y. Meng, G.F. Ning, L.J. Li, Fatigue performance of rubber-modified recycled aggregate concrete (RRAC) for pavement, Constr. Build. Mater. 95 (2015) 207–217, https://doi.org/10.1016/j.conbuildmat.2015.07.042.
[10] H.S. Shang, T.J. Zhao, W.Q. Cao, Bond behavior between steel bar and recycled aggregate concrete after freeze-thaw cycles, Cold Reg. Sci. Technol. 118 (2015) 38–44, https://doi.org/10.1016/j.coldregions.2015.06.008.
[11] R.V. Silva, R. Neves, J. De Brito, R.K. Dhir, Carbonation behaviour of recycled aggregate concrete, Cem. Concr. Compos. 62 (2015) 22–32, https://doi.org/10.1016/j.cemconcomp.2015.04.017.
[12] J. Davidovits, Geopolymer Chemistry and Applications, 4th ed, Institute Gèopolymère, Institut Géopolymère, 2015.
[13] C. Meyer, The greening of the concrete industry, Cem. Concr. Compos. 31 (2009) 601–605, https://doi.org/10.1016/j.cemconcomp.2008.12.010.
[14] W. Chalee Chindaprasirt, Effect of sodium hydroxide concentration on chloride penetration and steel corrosion of fly ash-based geopolymer concrete under marine site, Constr. Build. Mater. 63 (2014) 303–310, https://doi.org/10.1016/j.conbuildmat.2014.04.010.
[15] C. Gunasekara, D. Law, S. Bhuiyan, S. Setunge, L. Ward, Chloride induced corrosion in different fly ash based geopolymer concretes, Constr. Build. Mater. 200 (2019) 502–513, https://doi.org/10.1016/j.conbuildmat.2018.12.168.
[16] S. Luhar, S. Chaudhary, I. Luhar, Thermal resistance of fly ash based rubberized geopolymer concrete, J. Build. Eng. 19 (2018) 420–428, https://doi.org/10.1016/j.jobe.2018.05.025.
[17] Y. Fu, L. Cai, W. Yonggen, Freeze-thaw cycle test and damage mechanics models of alkali-activated slag concrete, Constr. Build. Mater. 25 (2011) 3144–3148, https://doi.org/10.1016/j.conbuildmat.2010.12.006.
[18] Y. Yuan, R. Zhao, R. Li, Y. Wang, Z. Cheng, F. Li, Z. John Ma, Frost resistance of fiber-reinforced blended slag and Class F fly ash-based geopolymer concrete under the coupling effect of freeze-thaw cycling and axial compressive loading, Constr. Build. Mater. 250 (2020) 118831, https://doi.org/10.1016/j.conbuildmat.2020.118831.
[19] N. Li, N. Farzadnia, C. Shi, Microstructural changes in alkali-activated slag mortars induced by accelerated carbonation, Cem. Concr. Res. 100 (2017) 214–226, https://doi.org/10.1016/j.cemconres.2017.07.008.

[20] S.A. Bernal, R. Mejía De Gutiérrez, A.L. Pedraza, J.L. Provis, E.D. Rodriguez, S. Delvasto, Effect of binder content on the performance of alkali-activated slag concretes, Cem. Concr. Res. 41 (2011) 1–8, https://doi.org/10.1016/j.cemconres.2010.08.017.
[21] M. Ibrahim, M.A. Megat Johari, M.K. Rahman, M. Maslehuddin, H.D. Mohamed, Enhancing the engineering properties and microstructure of room temperature cured alkali activated natural pozzolan based concrete utilizing nanosilica, Constr. Build. Mater. 189 (2018) 352–365, https://doi.org/10.1016/j.conbuildmat.2018.08.166.
[22] P. Nath, P.K. Sarker, Effect of GGBFS on setting, workability and early strength properties of fly ash geopolymer concrete cured in ambient condition, Constr. Build. Mater. 66 (2014) 163–171, https://doi.org/10.1016/j.conbuildmat.2014.05.080.
[23] A. Mehta, R. Siddique, Strength, permeability and micro-structural characteristics of low-calcium fly ash based geopolymers, Constr. Build. Mater. 141 (2017) 325–334, https://doi.org/10.1016/j.conbuildmat.2017.03.031.
[24] M. Sofi, J.S.J. van Deventer, P.A. Mendis, G.C. Lukey, Engineering properties of inorganic polymer concretes (IPCs), Cem. Concr. Res. 37 (2007) 251–257, https://doi.org/10.1016/j.cemconres.2006.10.008.
[25] Climate Analytics, Coal Phase-out: Insights from the IPCC Special Report on 1.5°C and Global Trends since 2015, 2019, pp. 3–6. https://climateanalytics.org/publications/2019/coal-phase-out-insights-from-the-ipcc-special-report-on-15c-and-global-trends-since-2015/.
[26] N.B. Singh, M. Kumar, S. Rai, Geopolymer cement and concrete: properties, Mater. Today Proc. 29 (2019) 743–748, https://doi.org/10.1016/j.matpr.2020.04.513.
[27] Department Of The Environment And Energy, 014 National Waste Report 2018, Blue Environ. Pty Ltd., 2018, pp. 1–126. https://www.environment.gov.au/system/files/resources/7381c1de-31d0-429b-912c-91a6dbc83af7/files/national-waste-report-2018.pdf.
[28] P. Jongpradist, W. Homtragoon, R. Sukkarak, W. Kongkitkul, P. Jamsawang, Efficiency of rice husk ash as cementitious material in high-strength cement-admixed clay, Adv. Civ. Eng. Mater. 2018 (2018), https://doi.org/10.1155/2018/8346319.
[29] B. Singh, Rice Husk Ash, Elsevier Ltd, 2018, https://doi.org/10.1016/B978-0-08-102156-9.00013-4.
[30] S.K. Das, J. Mishra, S.K. Singh, S.M. Mustakim, A. Patel, S.K. Das, U. Behera, Characterization and utilization of rice husk ash (RHA) in fly ash – blast furnace slag based geopolymer concrete for sustainable future, Mater. Today Proc. 33 (2020) 5162–5167, https://doi.org/10.1016/j.matpr.2020.02.870.
[31] M. Glavind, Sustainability of Cement, Concrete and Cement Replacement Materials in Construction, Woodhead Publishing Limited, 2009, https://doi.org/10.1533/9781845695842.120.
[32] Liang, Y. Ji, Mechanical properties and permeability of red mud-blast furnace slag-based geopolymer concrete, SN Appl. Sci. 3 (2021) 1–10, https://doi.org/10.1007/s42452-020-03985-4.
[33] C. Bobirică, J.H. Shim, J.H. Pyeon, J.Y. Park, Influence of waste glass on the microstructure and strength of inorganic polymers, Ceram. Int. 41 (2015) 13638–13649, https://doi.org/10.1016/j.ceramint.2015.07.160.
[34] J. He, Y. Jie, J. Zhang, Y. Yu, G. Zhang, Synthesis and characterization of red mud and rice husk ash-based geopolymer composites, Cem. Concr. Compos. 37 (2013) 108–118, https://doi.org/10.1016/j.cemconcomp.2012.11.010.
[35] C.L. Hwang, T.P. Huynh, Effect of alkali-activator and rice husk ash content on strength development of fly ash and residual rice husk ash-based geopolymers, Constr. Build. Mater. 101 (2015) 1–9, https://doi.org/10.1016/j.conbuildmat.2015.10.025.
[36] N. Li, C. Shi, Z. Zhang, D. Zhu, H.J. Hwang, Y. Zhu, T. Sun, A mixture proportioning method for the development of performance-based alkali-activated slag-based concrete, Cem. Concr. Compos. 93 (2018) 163–174, https://doi.org/10.1016/j.cemconcomp.2018.07.009.
[37] P. Zhang, Z. Gao, J. Wang, J. Guo, S. Hu, Y. Ling, Properties of fresh and hardened fly ash/slag based geopolymer concrete: a review, J. Clean. Prod. 270 (2020), https://doi.org/10.1016/j.jclepro.2020.122389.
[38] P. Chindaprasirt, C. Jaturapitakkul, W. Chalee, U. Rattanasak, Comparative study on the characteristics of fly ash and bottom ash geopolymers, Waste Manag. 29 (2009) 539–543, https://doi.org/10.1016/j.wasman.2008.06.023.
[39] P. Nuaklong, V. Sata, P. Chindaprasirt, Influence of recycled aggregate on fly ash geopolymer concrete properties, J. Clean. Prod. 112 (2016) 2300–2307, https://doi.org/10.1016/j.jclepro.2015.10.109.
[40] U. Rattanasak, K. Pankhet, P. Chindaprasirt, Effect of chemical admixtures on properties of high-calcium fly ash geopolymer, Int. J. Miner. Metall. Mater. 18 (2011) 364–369, https://doi.org/10.1007/s12613-011-0448-3.
[41] H. Xu, Q. Li, L. Shen, M. Zhang, J. Zhai, Low-reactive circulating fluidized bed combustion (CFBC) fly ashes as source material for geopolymer synthesis, Waste Manag. 30 (2010) 57–62, https://doi.org/10.1016/j.wasman.2009.09.014.
[42] S. Hanjitsuwan, S. Hunpratub, P. Thongbai, S. Maensiri, V. Sata, P. Chindaprasirt, Effects of NaOH concentrations on physical and electrical properties of high calcium fly ash geopolymer paste, Cem. Concr. Compos. 45 (2014) 9–14, https://doi.org/10.1016/j.cemconcomp.2013.09.012.
[43] U. Rattanasak, P. Chindaprasirt, Influence of NaOH solution on the synthesis of fly ash geopolymer, Miner. Eng. 22 (2009) 1073–1078, https://doi.org/10.1016/j.mineng.2009.03.022.
[44] L.N. Assi, E. (Eddie) Deaver, P. Ziehl, Using sucrose for improvement of initial and final setting times of silica fume-based activating solution of fly ash geopolymer concrete, Constr. Build. Mater. 191 (2018) 47–55, https://doi.org/10.1016/j.conbuildmat.2018.09.199.
[45] C.B. Cheah, M.H. Samsudin, M. Ramli, W.K. Part, L.E. Tan, The use of high calcium wood ash in the preparation of Ground Granulated Blast Furnace Slag and pulverized fly Ash geopolymers: a complete microstructural and mechanical characterization, J. Clean. Prod. 156 (2017) 114–123, https://doi.org/10.1016/j.jclepro.2017.04.026.
[46] S.M. Laskar, S. Talukdar, Preparation and tests for workability, compressive and bond strength of ultra-fine slag based geopolymer as concrete repairing agent, Constr. Build. Mater. 154 (2017) 176–190, https://doi.org/10.1016/j.conbuildmat.2017.07.187.
[47] Shang, J.G. Dai, T.J. Zhao, S.Y. Guo, P. Zhang, B. Mu, Alternation of traditional cement mortars using fly ash-based geopolymer mortars modified by slag, J. Clean. Prod. 203 (2018) 746–756, https://doi.org/10.1016/j.jclepro.2018.08.255.
[48] M. Venu, Gunneswara, Tie-confinement aspects of fly ash-GGBS based geopolymer concrete short columns, Constr. Build. Mater. 151 (2017) 28–35, https://doi.org/10.1016/j.conbuildmat.2017.06.065.
[49] R. Si, S. Guo, Q. Dai, J. Wang, Atomic-structure, microstructure and mechanical properties of glass powder modified metakaolin-based geopolymer, Constr. Build. Mater. 254 (2020), https://doi.org/10.1016/j.conbuildmat.2020.119303.
[50] J.X. Lu, C.S. Poon, Use of waste glass in alkali activated cement mortar, Constr. Build. Mater. 160 (2018) 399–407, https://doi.org/10.1016/j.conbuildmat.2017.11.080.
[51] C.C. Wang, H.Y. Wang, B.T. Chen, Y.C. Peng, Study on the engineering properties and prediction models of an alkali-activated mortar material containing recycled waste glass, Constr. Build. Mater. 132 (2017) 130–141, https://doi.org/10.1016/j.conbuildmat.2016.11.103.
[52] M. Vafaei, A. Allahverdi, High strength geopolymer binder based on waste-glass powder, Adv. Powder Technol. 28 (2017) 215–222, https://doi.org/10.1016/j.apt.2016.09.034.
[53] Parveen, D. Singhal, B.B. Jindal, Experimental study on geopolymer concrete prepared using high-silica RHA incorporating alccofine, Adv. Concr. Constr 5 (2017) 345–358, https://doi.org/10.12989/acc.2017.5.4.345.
[54] J. Xie, W. Chen, J. Wang, C. Fang, B. Zhang, F. Liu, Coupling effects of recycled aggregate and GGBS/metakaolin on physicochemical properties of geopolymer concrete, Constr. Build. Mater. 226 (2019) 345–359, https://doi.org/10.1016/j.conbuildmat.2019.07.311.
[55] A. Kumar, S. Kumar, Development of paving blocks from synergistic use of red mud and fly ash using geopolymerization, Constr. Build. Mater. 38 (2013) 865–871, https://doi.org/10.1016/j.conbuildmat.2012.09.013.
[56] K.L. Lin, H.S. Shiu, J.L. Shie, T.W. Cheng, C.L. Hwang, Effect of composition on characteristics of thin film transistor liquid crystal display (TFT-LCD) waste glass-metakaolin-based geopolymers, Constr. Build. Mater. 36 (2012) 501–507, https://doi.org/10.1016/j.conbuildmat.2012.05.018.
[57] E.I. Diaz, E.N. Allouche, S. Eklund, Factors affecting the suitability of fly ash as source material for geopolymers, Fuel. 89 (2010) 992–996, https://doi.org/10.1016/j.fuel.2009.09.012.
[58] D. Hardjito, S.E. Wallah, D.M.J. Sumajouw, B.V. Rangan, On the development of fly ash-based geopolymer concrete, ACI Mater. J. 101 (2004) 467–472, https://doi.org/10.14359/13485.

[59] N. Li, C. Shi, Z. Zhang, H. Wang, Y. Liu, A review on mixture design methods for geopolymer concrete, Compos. Part B Eng. 178 (2019) 107490, https://doi.org/10.1016/j.compositesb.2019.107490.

[60] K. Pimraksa, P. Chindaprasirt, A. Rungchet, K. Sagoe-Crentsil, T. Sato, Lightweight geopolymer made of highly porous siliceous materials with various Na2O/Al2O3 and SiO2/Al2O3 ratios, Mater. Sci. Eng. A. 528 (2011) 6616–6623, https://doi.org/10.1016/j.msea.2011.04.044.

[61] M. Torres-Carrasco, F. Puertas, Waste glass in the geopolymer preparation. Mechanical and microstructural characterisation, J. Clean. Prod. 90 (2015) 397–408, https://doi.org/10.1016/j.jclepro.2014.11.074.

[62] S. Alonso, A. Palomo, Alkaline activation of metakaolin and calcium hydroxide mixtures: influence of temperature, activator concentration and solids ratio, Mater. Lett. 47 (2001) 55–62, https://doi.org/10.1016/S0167-577X(00)00212-3.

[63] M.N.S. Hadi, H. Zhang, S. Parkinson, Optimum mix design of geopolymer pastes and concretes cured in ambient condition based on compressive strength, setting time and workability, J. Build. Eng. 23 (2019) 301–313, https://doi.org/10.1016/j.jobe.2019.02.006.

[64] P. Pavithra, M. Srinivasula Reddy, P. Dinakar, B. Hanumantha Rao, B.K. Satpathy, A.N. Mohanty, A mix design procedure for geopolymer concrete with fly ash, J. Clean. Prod. 133 (2016) 117–125, https://doi.org/10.1016/j.jclepro.2016.05.041.

[65] P. Duxson, J.L. Provis, G.C. Lukey, S.W. Mallicoat, W.M. Kriven, J.S.J. Van Deventer, Understanding the relationship between geopolymer composition, microstructure and mechanical properties, Colloids Surf. A Physicochem. Eng. Asp. 269 (2005) 47–58, https://doi.org/10.1016/j.colsurfa.2005.06.060.

[66] R. Redden, N. Neithalath, Microstructure, strength, and moisture stability of alkali activated glass powder-based binders, Cem. Concr. Compos. 45 (2014) 46–56, https://doi.org/10.1016/j.cemconcomp.2013.09.011.

[67] Mehta, R. Siddique, Sustainable geopolymer concrete using ground granulated blast furnace slag and rice husk ash: strength and permeability properties, J. Clean. Prod. 205 (2018) 49–57, https://doi.org/10.1016/j.jclepro.2018.08.313.

[68] D. Yan, S. Chen, Q. Zeng, S. Xu, H. Li, Correlating the elastic properties of metakaolin-based geopolymer with its composition, Mater. Des. 95 (2016) 306–318, https://doi.org/10.1016/j.matdes.2016.01.107.

[69] R.M. Novais, G. Ascensão, M.P. Seabra, J.A. Labrincha, Waste glass from end-of-life fluorescent lamps as raw material in geopolymers, Waste Manag. 52 (2016) 245–255, https://doi.org/10.1016/j.wasman.2016.04.003.

[70] I. Ozer, S. Soyer-Uzun, Relations between the structural characteristics and compressive strength in metakaolin based geopolymers with different molar Si/Al ratios, Ceram. Int. 41 (2015) 10192–10198, https://doi.org/10.1016/j.ceramint.2015.04.125.

[71] C. Gunasekara, D.W. Law, S. Setunge, Long term permeation properties of different fly ash geopolymer concretes, Constr. Build. Mater. 124 (2016) 352–362, https://doi.org/10.1016/j.conbuildmat.2016.07.121.

[72] J.L. Provis, J.S.J. Van Deventer, Introduction to Geopolymers, Woodhead Publishing Limited, 2009, https://doi.org/10.1533/9781845696382.1.

[73] A.B. Pascual, M.T. Tognonvi, A. Tagnit-Hamou, Waste glass powder-based alkali-activated mortar, Int. J. Res. Eng. Technol. 03 (2014) 32–36, https://doi.org/10.15623/ijret.2014.0325006.

[74] H. Rahier, J.F. Denayer, B. Van Mele, Low-temperature synthesized aluminosilicate glasses: part IV. Modulated DSC study on the effect of particle size of metakaolinite on the production of inorganic polymer glasses, J. Mater. Sci. 38 (2003) 3131–3136, https://doi.org/10.1023/A:1024733431657.

[75] A. Kusbiantoro, M.F. Nuruddin, N. Shafiq, S.A. Qazi, The effect of microwave incinerated rice husk ash on the compressive and bond strength of fly ash based geopolymer concrete, Constr. Build. Mater. 36 (2012) 695–703, https://doi.org/10.1016/j.conbuildmat.2012.06.064.

[76] M.N.S. Hadi, N.A. Farhan, M.N. Sheikh, Design of geopolymer concrete with GGBFS at ambient curing condition using Taguchi method, Constr. Build. Mater. 140 (2017) 424–431, https://doi.org/10.1016/j.conbuildmat.2017.02.131.

[77] X. Chen, Y. Guo, S. Ding, H. Zhang, F. Xia, J. Wang, M. Zhou, Utilization of red mud in geopolymer-based pervious concrete with function of adsorption of heavy metal ions, J. Clean. Prod. 207 (2019) 789–800, https://doi.org/10.1016/j.jclepro.2018.09.263.

[78] G. Liu, M.V.A. Florea, H.J.H. Brouwers, Waste glass as binder in alkali activated slag–fly ash mortars, Mater. Struct. Constr. 52 (2019), https://doi.org/10.1617/s11527-019-1404-3.

[79] G.N. Kishore, B. Gayathri, Experimental study on rise husk ash & fly ash based geo-polymer concrete using M-Sand, in: IOP Conf. Ser. Mater. Sci. Eng., Institute of Physics Publishing, 2017 https://doi.org/10.1088/1757-899X/225/1/012273.

[80] G. Liang, H. Zhu, Z. Zhang, Q. Wu, Effect of rice husk ash addition on the compressive strength and thermal stability of metakaolin based geopolymer, Constr. Build. Mater. 222 (2019) 872–881, https://doi.org/10.1016/j.conbuildmat.2019.06.200.

[81] A.M. Fernández-Jiménez, A. Palomo, C. López-Hombrados, Engineering properties of alkali-activated fly ash concrete, ACI Mater. J. 103 (2006) 106–112, https://doi.org/10.14359/15261.

[82] F. Puertas, T. Amat, A. Fernández-Jiménez, T. Vázquez, Mechanical and durable behaviour of alkaline cement mortars reinforced with polypropylene fibres, Cem. Concr. Res. 33 (2003) 2031–2036, https://doi.org/10.1016/S0008-8846(03)00222-9.

[83] D. Bondar, C.J. Lynsdale, N.B. Milestone, N. Hassani, A.A. Ramezanianpour, Engineering properties of alkali activated natural pozzolan concrete, 2nd Int. Conf. Sustain. Constr. Mater. Technol. (2010) 1093–1102, https://doi.org/10.14359/51664217.

[84] P. Nath, P.K. Sarker, Flexural strength and elastic modulus of ambient-cured blended low-calcium fly ash geopolymer concrete, Constr. Build. Mater. 130 (2017) 22–31, https://doi.org/10.1016/j.conbuildmat.2016.11.034.

[85] B.A. Latella, D.S. Perera, D. Durce, E.G. Mehrtens, J. Davis, Mechanical properties of metakaolin-based geopolymers with molar ratios of Si/Al ≈ 2 and Na/Al ≈ 1, J. Mater. Sci. 43 (2008) 2693–2699, https://doi.org/10.1007/s10853-007-2412-1.

[86] C. Bobirică, C. Orbeci, L. Bobirică, P. Palade, C. Deleanu, C.M. Pantilimon, C. Pîrvu, I.C. Radu, Influence of red mud and waste glass on the microstructure, strength, and leaching behavior of bottom ash-based geopolymer composites, Sci. Rep. 10 (2020), https://doi.org/10.1038/s41598-020-76818-4.

[87] B.B. Jindal, P. Jangra, A. Garg, Effects of ultra fine slag as mineral admixture on the compressive strength, water absorption and permeability of rice husk ash based geopolymer concrete. Mater. Today Proc., Elsevier Ltd, 2020, pp. 871–877, https://doi.org/10.1016/j.matpr.2020.04.219.

[88] K. Kupwade-Patil, E.N. Allouche, Impact of alkali silica reaction on fly ash-based geopolymer concrete, J. Mater. Civ. Eng. 25 (2013) 131–139, https://doi.org/10.1061/(asce)mt.1943-5533.0000579.

[89] R. Pouhet, M. Cyr, Alkali–silica reaction in metakaolin-based geopolymer mortar, Mater. Struct. Constr. 48 (2014) 571–583, https://doi.org/10.1617/s11527-014-0445-x.

[90] T. Williamson, M.C.G. Juenger, The role of activating solution concentration on alkali-silica reaction in alkali-activated fly ash concrete, Cem. Concr. Res. 83 (2016) 124–130, https://doi.org/10.1016/j.cemconres.2016.02.008.

[91] M. Yang, S.R. Paudel, E. Asa, Comparison of pore structure in alkali activated fly ash geopolymer and ordinary concrete due to alkali-silica reaction using micro-computed tomography, Constr. Build. Mater. 236 (2020) 117524, https://doi.org/10.1016/j.conbuildmat.2019.117524.

[92] R. Tänzer, Y. Jin, D. Stephan, Effect of the inherent alkalis of alkali activated slag on the risk of alkali silica reaction, Cem. Concr. Res. 98 (2017) 82–90, https://doi.org/10.1016/j.cemconres.2017.04.009.

[93] A. Omran, A. Tagnit-Hamou, Performance of glass-powder concrete in field applications, Constr. Build. Mater. 109 (2016) 84–95, https://doi.org/10.1016/j.conbuildmat.2016.02.006.

[94] Y. Shao, T. Lefort, S. Moras, D. Rodriguez, Studies on concrete containing ground waste glass, Cem. Concr. Res. 30 (2000) 91–100, https://doi.org/10.1016/S0008-8846(99)00213-6.

[95] A. Shayan, A. Xu, Value-added utilisation of waste glass in concrete, Cem. Concr. Res. 34 (2004) 81–89, https://doi.org/10.1016/S0008-8846(03)00251-5.

[96] C. Shi, Y. Wu, C. Riefler, H. Wang, Characteristics and pozzolanic reactivity of glass powders, Cem. Concr. Res. 35 (2005) 987–993, https://doi.org/10.1016/j.cemconres.2004.05.015.

[97] O.F. Nnaemeka, N.B. Singh, Durability properties of geopolymer concrete made from fly ash in presence of Kaolin, Mater. Today Proc. 29 (2019) 781–784, https://doi.org/10.1016/j.matpr.2020.04.696.

[98] M.B. Karakoç, I. Türkmen, M.M. Maraş, F. Kantarci, R. Demirboła, Sulfate resistance of ferrochrome slag based geopolymer concrete, Ceram. Int. 42 (2016) 1254–1260, https://doi.org/10.1016/j.ceramint.2015.09.058.

[99] N. Ganesan, R. Abraham, S. Deepa Raj, Durability characteristics of steel fibre reinforced geopolymer concrete, Constr. Build. Mater. 93 (2015) 471–476, https://doi.org/10.1016/j.conbuildmat.2015.06.014.
[100] M. Olivia, H. Nikraz, Durability of Fly Ash Geopolymer Concrete in a Seawater Environment, Concr. 2011. 25th Bienn. …., 2011. http://espace.library.curtin.edu.au/cgi-bin/espace.pdf?file=/2011/10/27/file_1/167459.
[101] A. Noushini, A. Castel, J. Aldred, A. Rawal, Chloride diffusion resistance and chloride binding capacity of fly ash-based geopolymer concrete, Cem. Concr. Compos. 105 (2020) 103290, https://doi.org/10.1016/j.cemconcomp.2019.04.006.
[102] M. Kamali, A. Ghahremaninezhad, Effect of glass powders on the mechanical and durability properties of cementitious materials, Constr. Build. Mater. 98 (2015) 407–416, https://doi.org/10.1016/j.conbuildmat.2015.06.010.
[103] H. Siad, M. Lachemi, M. Sahmaran, K.M.A. Hossain, Effect of glass powder on sulfuric acid resistance of cementitious materials, Constr. Build. Mater. 113 (2015) 163–173, https://doi.org/10.1016/j.conbuildmat.2016.03.049.
[104] M.N.N. Khan, J.C. Kuri, P.K. Sarker, Effect of waste glass powder as a partial precursor in ambient cured alkali activated fly ash and fly ash-GGBFS mortars, J. Build. Eng. 34 (2021) 101934, https://doi.org/10.1016/j.jobe.2020.101934.
[105] B. Parthiban, S. Thirugnanasambandam, Eco-friendly geopolymer concrete using recycled waste glass as fine aggregate, Int. J. Recent Sci. Res. 9 (2018) 29660–29664, https://doi.org/10.24327/IJRSR.
[106] N.S. Júnior, J.S. Andrade Neto, H.A. Santana, M.S. Cilla, D.V. Ribeiro, Durability and service life analysis of metakaolin-based geopolymer concretes with respect to chloride penetration using chloride migration test and corrosion potential, Constr. Build. Mater. 287 (2021), https://doi.org/10.1016/j.conbuildmat.2021.122970.